THE JOURNAL OF PHYSICAL CHEMISTRY A

Article

pubs.acs.org/JPCA

Slow Photoelectron Velocity-Map Imaging Spectroscopy of Cold Thiozonide (S_3^-)

Jongjin B. Kim, Christian Hock,[†] Tara I. Yacovitch,[‡] and Daniel M. Neumark*

Department of Chemistry, University of California, Berkeley, California 94720, United States, and Chemical Sciences Division, Lawrence Berkeley National Laboratory, Berkeley, California 94720, United States

ABSTRACT: We report high-resolution anion photoelectron spectra of thiozonide (S_3^-) acquired by slow electron velocity-map imaging (SEVI). The ions were cryogenically cooled within an ion trap before photodetachment. We measure an electron affinity of 2.3630(9) eV, resolving discrepancies in previously reported photoelectron spectra that resulted from the presence of vibrational hot bands. The SEVI spectrum shows well-resolved, extended vibrational progressions in the symmetric stretch and bending modes of S_3, yielding accurate frequencies for both.

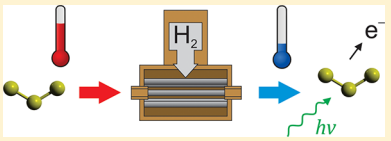

INTRODUCTION

With the possible exception of carbon, sulfur has more complex allotropy than any other element.[1] In addition to the numerous cyclic and polymeric forms in the solid and liquid phases, sulfur vapor is composed of the species S_n ($2 \leq n \leq 8$), with trace amounts of S_9 and S_{10}.[2] Aside from the diatomic S_2, S_3 has received the most attention of these species. Its relatively small size makes it accessible to experiment and theory, and additional interest comes about because S_3 is isovalent with ozone. It has been studied by rare gas matrix IR and UV−vis spectroscopy,[3,4] resonance Raman in the gas phase,[5,6] microwave spectroscopy,[7,8] photoionization,[9] and gas-phase absorption.[10] Ab initio calculations on S_3 have focused on the question of whether the cyclic D_{3h} or the bent C_{2v} structure is the lowest-energy isomer,[11−14] finding overall agreement with experiment that the C_{2v} form is the stable form. High-level calculations on the structure, vibrations, and excited states of S_3 have recently been reported by Francisco et al.[15,16]

In contrast to neutral S_3, work on the S_3^- anion has largely been limited to spectroscopy in condensed phases, where it has been studied by electron paramagnetic resonance (EPR), Raman, and absorption spectroscopy.[17−19] As it is the chromophore in ultramarine pigment,[20] many of these investigations were focused on determining the properties of S_3^- in a perturbative mineral matrix or in solution. In addition, electronic absorption spectra have been measured in a cryogenic rare gas matrix.[21] Recently, the anion has been identified as the dominant form of sulfur in certain high-pressure and temperature conditions approximating crustal and subduction-zone geologic fluids.[22] The new findings suggest that S_3^- may play an important role in the transport of sulfur and chalcophile metals in the earth.

The neutral ← anion transition has been studied by anion photoelectron spectroscopy (PES) with resolution sufficient to resolve a progression of the ν_1 symmetric stretch.[23−25] However, the two previous studies disagreed over which peak in this progression was the vibrational origin. By assuming the anions were at the ground vibrational state, Nimlos et al.[23] obtained an electron affinity (EA) of 2.106(23) eV. Hunsicker et al.[24] found a different onset for the band, suggesting the possibility that the two experiments produced anions with different vibrational temperatures and that some of the low binding energy peaks came from hot bands. They narrowed down the likely 0−0 transitions, giving a possible EA ranging from 2.33 to 2.40 eV.

In this article, we report high-resolution photoelectron spectra via slow electron velocity-map imaging (SEVI) of cryogenically cooled S_3^-, eliminating any ambiguity over the initial anion temperature and clearly identifying the 0_0^0 transition. An additional ν_2 bend progression is resolved, and the spectrum is compared to a Franck−Condon simulation with good agreement. The EA is identified as 2.3630(9) eV, and the ν_2 frequency obtained is 260(2) cm^{-1}, lower than previously reported[6] for gas phase S_3.

EXPERIMENTAL SECTION

The experimental setup has been described in detail previously.[26−28] Ions were cooled to their vibrational ground state in an ion trap. They were then mass-selected and photodetached with a tunable dye laser. The ejected photoelectrons were analyzed with a velocity-map imaging spectrometer with low extraction voltages, such that slow electrons were collected and energy-analyzed with high resolution. Spectra were recorded at different photon energies and combined to create a high-resolution spectrum over a wider range.

Ions were produced by a pulsed solenoid valve coupled to a ring ionizer. Solid sulfur powder was heated to 80 °C and its vapor entrained in 300 psi of argon buffer gas, which was then expanded into vacuum through an Even−Lavie pulsed valve.[29] The neutral sulfur vapor clusters were bombarded by electrons from a ring ionizer, causing fragmentation and ionization. The

Special Issue: Stereodynamics Symposium

Received: January 30, 2013
Revised: March 4, 2013
Published: March 5, 2013

   dx.doi.org/10.1021/jp401083u | J. Phys. Chem. A 2013, 117, 8126−8131

resulting ions were transferred through a series of radio frequency (RF) ion guides into a linear octupole ion trap. Ions were confined within the trap by RF fields applied to the trap rods[30] and DC voltages on entrance and exit electrodes. The trap was in thermal contact with a closed-cycle refrigerator and was cooled down to 35 K. (Lower temperatures using a more powerful refrigerator are now available to us.[27]) While the ions were stored in the ion trap for ~45 ms, H_2 buffer gas was continuously injected into the ion trap through a variable leak valve. He was also used as a buffer gas but was less effective than H_2 in cooling S_3^-. The buffer gas thermalized the ions, cooling the ions close to the trap temperature of 35 K. Under these conditions, the ions should be in their vibrational ground state; the lowest-frequency ν_2 mode of the anion has been measured to be around 230 cm^{-1},[17,18] so the equilibrium excited state population should be <0.1%.

After cooling in the trap, the ions were transferred to an orthogonal time-of-flight mass spectrometer that temporally and spatially focuses mass-selected $^{32}S_3^-$ into the laser interaction region of the SEVI electron energy spectrometer. Here, the ion packets were photodetached with the output from a Nd:YAG-pumped tunable dye laser. The resulting photoelectrons were focused with a velocity-map imaging (VMI) electrostatic lens to an imaging detector,[31] comprising a chevron-stacked pair of microchannel plates coupled to a phosphor screen, with the resulting image recorded by a CCD camera.

The projected 2D images were transformed to reconstruct the original 3D electron velocity distribution, using the inverse-Abel algorithm of Hansen and Law.[32] Under the VMI focusing conditions, the radius of the electron distribution is proportional to its speed, which in turn is proportional to the square root of the kinetic energy. As all transitions have similar widths in image space, transitions with slow photoelectrons have the best energy resolution. Thus, to obtain the best resolution for all transitions of interest, the laser frequency was moved to take spectra at different photon energies, while the VMI voltages were chosen so the electron kinetic energy window was ~4000 cm^{-1} . Spectra are reported in electron binding energy (eBE), given by the difference between the photon energy and the measured electron kinetic energy. As in previous work on sulfur-containing anions,[33] the VMI spectrometer was calibrated by recording spectra of the well-characterized transitions of S^- photodetachment.[34]

CALCULATIONS

Electronic structure calculations were run at the RCCSD(T)/aug-cc-pV(Q+d)Z level of theory to determine the energies, geometries, harmonic frequencies, and normal modes of the $^2B_1$ anion and $^1A_1$ neutral S_3 species.[35−37] All electronic structure calculations were run using Molpro 2010.1.[38] Geometries were restricted to C_{2v} symmetry, in keeping with previous experimental and theoretical conclusions.[8,15,20,24]

Franck−Condon (FC) simulations for the neutral ← anion transitions were carried out with the ezSpectrum program.[39] The simulations calculated FC overlap treating all modes as harmonic oscillators, using full Duschinsky mixing of the normal modes to map the initial to final coordinates.[40] The position of the 0_0^0 transition was fixed at the experimentally assigned adiabatic transition, and frequencies of the neutral were set to match experimental values. As the structure of S_3 has been experimentally determined by microwave spectroscopy,[8] the anion geometry was adjusted so that the simulated spectrum fit the experimental spectrum.

RESULTS

SEVI spectra of thiozonide taken under different cooling conditions are presented in Figure 1. The spectra in Figure 1

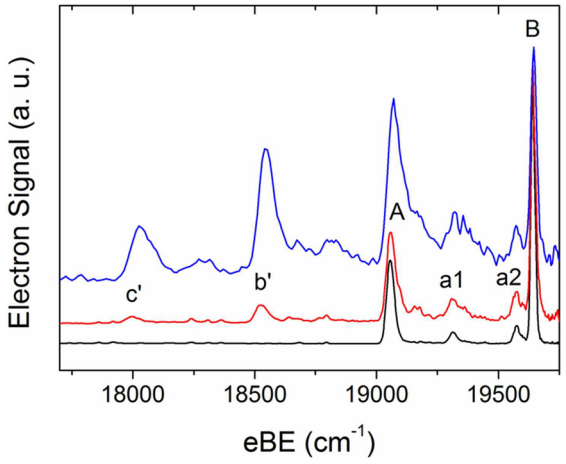

Figure 1. SEVI spectra of thiozonide showing the transition from the $^2B_1$ state of S_3^- to the $^1A_1$ state of S_3 under differing experimental conditions. The top blue trace shows a scan before the trap was installed. The intermediate red trace shows a scan taken with He as the buffer gas in the ion trap, and the bottom black trace was taken under identical conditions, but with H_2 as the buffer gas.

were taken at a frequency of 19 776 cm^{-1}. The top spectrum (blue) was taken before the installation of the trap, the middle (red) was taken with He buffer gas in the 35 K ion trap, and the bottom (black) was with H_2 as the buffer gas, with all three normalized to the same height for peak B, then offset vertically for illustration. Because of the limited electron kinetic energy window, the lower energy was chosen to emphasize the low-eBE peaks b′ and c′ and how their relative intensities change upon different cooling conditions.

Figure 2 shows more data taken with H_2 buffer gas: an overview spectrum (blue) taken at a laser frequency of 22892

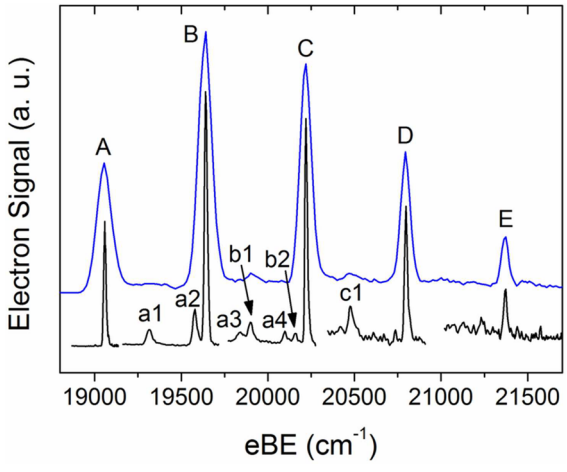

Figure 2. SEVI spectra of thiozonide showing the transition from the $^2B_1$ state of S_3^- to the $^1A_1$ state of S_3. The upper blue trace shows a low-resolution overview scan. The lower traces are high-resolution scans covering the range of the overview scan.

dx.doi.org/10.1021/jp401083u | J. Phys. Chem. A 2013, 117, 8126−8131

cm^{-1} and a composite spectrum (black) taken at several laser frequencies that were chosen to optimize energy resolution, with the individual segments scaled vertically to match the corresponding peaks in the overview spectrum. Typical peak widths are 16 cm^{-1} fwhm. The photoelectron angular distribution is described by the standard expression[41]

$$I(\theta) = \frac{\sigma}{4\pi}(1 + \beta P_2(\cos\theta)) \quad (1)$$

where θ is the angle between the photoelectron and the laser polarization axis. We find $\beta < 0$ for all transitions, consistent with electron detachment from the b_1 molecular orbital of S_3^-.[42]

Peak positions and assignments (see below) are summarized in Table 1. Calculated geometries, frequencies, and the EA are listed in Table 2, along with experimental values obtained here. As the resolution is limited by the unresolved rotational profile of each vibronic transition, peak uncertainties are reported by one standard deviation of a Gaussian fit to each peak in the composite spectrum in Figure 2, 7 cm^{-1} in this experiment. Peaks b′ and c′ in Figure 1 were acquired farther from threshold and at a hotter ion temperature and have a larger uncertainty of 25 cm^{-1}. All features below 19 000 cm^{-1} are suppressed upon ion trap cooling, suggesting that peak A is the vibrational origin. While the spectrum with H_2 cooling has no visible features at lower eBE than peak A, peaks b′ and c′ are still visible with He cooling and comprise a progression with peak A spaced by 530 cm^{-1}.

Table 1. Peak Positions (cm^{-1}), Shifts from the Origin (cm^{-1}), and Vibrational Assignments for the Thiozonide SEVI Spectra

peak	position	shift	assignment
c′	18001	−1058	1_2^0
b′	18530	−529	1_1^0
A	19059	0	0_0^0
a1	19316	257	2_0^1
a2	19579	520	2_0^2
B	19642	583	1_0^1
a3	19842	783	2_0^3
b1	19899	840	$1_0^1 2_0^1$
a4	20098	1039	2_0^4
b2	20157	1098	$1_0^1 2_0^2$
C	20221	1162	1_0^2
c1	20481	1422	$1_0^2 2_0^1$
D	20798	1739	1_0^3
E	21372	2313	1_0^4

Table 2. Calculated Bond Length (Å), Bond Angle (deg), Harmonic Frequencies (cm^{-1}), and Electron Affinity (cm^{-1}) for the Neutral and Anion Thiozone, at the CCSD(T)/aug-cc-pV(Q+d)Z Level; Experimental Values Obtained in This Work Are Also Included

	S_3^-		S_3	
	calcd	exptl	calcd	exptl
$R(SS)$	1.992	1.98(1)	1.920	
$\theta(SSS)$	115.0	114(1)	117.5	
ω_1	544	529(11)	595	584(6)
ω_2	230		262	260(2)
ω_3	610		696	
EA			19222	19059(7)

The spectra in Figure 2 are dominated by a single progression of peaks A−E, with a spacing of 580 cm^{-1}. There is a weaker progression of peaks a1−c1 with the same spacing but higher in energy by 260 cm^{-1} than peaks A−C. High-resolution scans show additional structure of peaks a2−a4 and b2, with a1−a4 and b1−b4 both comprising a series of peaks spaced by 260 cm^{-1}. Peaks b′ and c′ are absent in the spectra taken with hydrogen gas.

DISCUSSION

Previous PE experiments obtained at a resolution of 20−30 meV showed a series of peaks spaced by 500−600 cm^{-1} that was assigned to the ν_1 symmetric stretch progression,[23−25] but the vibrational origin transition could not be definitively identified. Nimlos et al.[23] assumed the peak at the lowest eBE was the 0_0^0 transition, yielding an EA of 2.093(25) eV. However, the apparent band origin in more recent work by Hunsicker et al.[24] appeared at a higher eBE, leading them to propose that some of the previously seen low-eBE peaks could be 1_n^0 hot bands. As the frequencies of the ν_1 anion and neutral modes are expected to differ by less than 50 cm^{-1},[5,6,17,18] the lower resolution of those experiments meant that they were unable to separate 1_n^0 hot bands from the main 1_0^n sequence by a shift in the spacing of the ν_1 progression. Furthermore, neither experiment had a reliable method to establish the vibrational temperature of the ions. Nimlos et al. did not cool the ions after production from a discharge and with this source have observed vibrational hot bands in other systems,[43] including an estimated vibrational temperature of 1000 K for Si_2^-.[44] Although Hunsicker et al. cooled their ions with a supersonic gas expansion, they have measured a vibrational temperature of ∼580 K for P_2^- with the same ion source,[45] so hot bands may also be present in their S_3^- experiment.

The higher resolution of SEVI compared to conventional PES should facilitate vibrational assignments, but Figure 1 shows that similar problems regarding vibrational temperature remain for S_3^-. The top trace in Figure 1 was acquired using the same pulsed, free-jet source with a ring ionizer for S_3^- before the installation of the ion trap. This spectrum is dominated by the ν_1 progression and shows additional smaller peaks between the main features. It thus represents a considerable improvement over the PE spectra, but there are indications that the ions are still vibrationally hot, making it difficult to assign the vibrational origin. Specifically, the peaks in the S_3^- spectrum are ∼100 cm^{-1} wide and quite asymmetric, suggesting unresolved spectral congestion from vibrational and rotational excitation. SEVI spectra of other anions taken with the same source yield much narrower peaks (<25 cm^{-1});[46,47] it appears that S_3^- is particularly difficult to cool in a free jet expansion.

The addition of ion trapping and cooling to SEVI should fix this problem by ensuring a specific vibrational temperature. As the ions are spatially confined in an RF trap, they are thermalized for tens of milliseconds with cryogenic buffer gas, allowing for more effective cooling of ions. This technique has been successfully used in many groups to cool ions to the ground vibrational state, including cluster species.[30,48−52] In particular, with our instrument, we have shown that we can cool C_5^- ions down to 10 K with a cold head at 5 K, with total quenching of all hot bands and sequence bands.[27] As shown in Figure 1, with helium as the buffer gas in a 35 K trap, peaks b′

dx.doi.org/10.1021/jp401083u | J. Phys. Chem. A 2013, 117, 8126−8131

and c′ are suppressed relative to peaks A and B, suggesting that peak A is the 0_0^0 transition and that b′ and c′ are the 1_1^0 and 1_2^0 transitions, respectively. The peak widths also get narrower, presumably due to fewer sequence bands and narrower rotational profiles.

At thermal equilibrium in a 35 K ion trap, peaks b′ and c′ should not be seen, but they are still observed with helium as the buffer gas. However, upon changing the gas to hydrogen, they are not observed above the background noise. Presumably, the additional rotational and vibrational degrees of freedom for H_2 result in more collisional cooling with vibrationally excited S_3^- produced by the ion source. As the H_2 fundamental is 4161 cm^{-1},[53] far in excess of any observed S_3^- vibrational excitation, vibration-to-rotation (V−R) energy transfer is likely to be the dominant additional cooling channel. Compared to He cooling, the line widths are further decreased, and peak A is unambiguously assigned as the adiabatic transition, giving S_3 an EA of 2.3630(9) eV.

With thiozonide cooled to its ground vibrational state, assignment of the other peaks is straightforward. According to the calculations, both the bond angle and bond lengths change upon photodetachment, so both the ν_1 stretch and ν_2 bend should be FC active. As in the previous two studies, peaks A−E are assigned to the 1_0^n progression; the 580 cm^{-1} spacing is in good agreement to the calculated harmonic frequency of 595 cm^{-1}.

Peaks a1−c1 appear at 260 cm^{-1} above peaks A−C, respectively. This is close to the calculated value of 262 cm^{-1} for the ν_2 mode, thus peaks a1−c1 are assigned to the $1_0^n2_0^1$ progression. Similarly, a1−a4 is the 2_0^n (n = 1−4) progression, while b1 and b2 are assigned to the $1_0^12_0^1$ and $1_0^12_0^2$ transitions, respectively.

Since the geometry of the neutral is known, the Franck−Condon fit can yield a quantitative measure for the geometry of the S_3^- anion. To fit the simulation to the overview spectrum, the stick spectrum was convolved with Gaussians with a relative kinetic energy resolution of 3%, typical of this experiment. The bond length and bond angle of the neutral were fixed to 1.917 Å and 117.36°,[8] respectively, and the anion geometry was adjusted for a best fit and the vibrational temperature set to 0 K. The best match was found at an anion bond length of 1.98(1) Å and a bond angle of 114(1)°, compared to calculated values of 1.992 Å and 115.0°, respectively. As shown in Figure 3, the simulation fits the overview very well. By comparison, the FC simulation with the ab initio geometries has a qualitatively similar 1_0^n progression, but negligible intensity in the ν_2 mode.

With the simulation parameters, the anion temperature can be adjusted so that the simulations reproduce the hot spectra in Figure 1. By doing so, the estimated vibrational temperatures are ∼1300 K with no cooling, ∼450 K with He gas, and <80 K with H_2. Ion trap cooling, and in this case particularly with H_2, can dramatically reduce the temperature of ions and simplify their spectra.

Although the simulation fits the overview spectrum quite well, including the small $1_0^n2_0^1$ peaks that lie between the peaks of the main 1_0^n progression, comparison with the high-resolution composite spectrum shows that it underestimates the intensities of transitions to more highly excited bend levels (a2−a4, b2) that are not resolved in the overview spectrum. This situation cannot be fixed by adjusting the simulation parameters; in a FC simulation, peak a2 cannot be made larger than a1 without both being less intense than the peak A, the band origin. One must also consider possible intensity

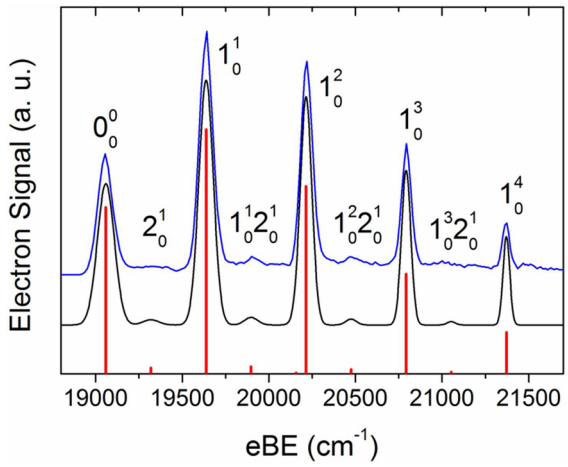

Figure 3. Stick spectrum of FC simulation (red), with labeled transitions. Spectrum broadened by instrument resolution is above (black), with the overview spectrum (blue) on top for comparison.

distortions in the high-resolution spectrum from the Wigner threshold law,[54] which generally reduces the intensity of features closer to their detachment threshold relative to those further away (i.e., lower eBE at the same photodetachment wavelength). However, this effect cannot explain why a1 is less intense than a2 since both were taken as part of the same scan. It may well be that a2 borrows intensity from the very intense peak B via a Fermi resonance between the upper levels for the two transitions, which are separated by only 60 cm^{-1}. In any case, this example illustrates that the high-resolution intrinsic to SEVI poses challenges when trying to simulate intensity distributions because one observes discrepancies that are simply not seen in conventional PE spectra.

Regardless of these small intensity anomalies, the peak assignments are unambiguous and yield frequencies for the ν_1 and ν_2 vibrations. By fitting the 1_0^n progression (peaks B−E) to a Morse potential and taking the peak uncertainties into account, the value for the neutral ν_1 fundamental and harmonic frequency is 583(5) cm^{-1} and 584(6) cm^{-1}, respectively. These are in good agreement with the values obtained by gas-phase resonance Raman spectroscopy of 581 cm^{-1} and 583.5 cm^{-1}, respectively.[6] The anion ν_1 harmonic frequency is determined to be 529(11) cm^{-1} by fitting b′ and c′ to a harmonic potential, consistent with values around 530 cm^{-1} in solution by resonance Raman.[17,18] Similarly, by fitting the 2_0^n progression (peaks a1−a4), the value of the neutral ν_2 fundamental is determined to be 260(2) cm^{-1}, and the harmonic frequency is the same within experimental error.

This last determination disagrees with the resonance Raman work of Picquenard et al.,[6] who assigned a value of 281 cm^{-1} for the ν_2 fundamental and 284.5 cm^{-1} for the harmonic frequency. Their assignment was based on an assignment of multiple peaks clustered around 260 cm^{-1}. The resonance Raman spectra were measured in a gas cell with sulfur vapor, and to have sufficient concentration of the S_3 allotrope, the temperature was raised to 630 °C, hot enough to have significant vibrational excitation of the target species. As a result, the Raman spectra were congested with many contributions from combination bands from molecules not in their ground vibrational state. Thus, the choice of which vibrational combination contributes to which peak is not obvious, and assignments were carried out with the aid of ^{34}S

dx.doi.org/10.1021/jp401083u | J. Phys. Chem. A 2013, 117, 8126−8131

isotopic substitution, but still with considerable ambiguity, due to uncertain isotopomer contributions, FC factors, and vibrational excitation. An earlier investigation by the same group tentatively assigned the dominant feature near 260 cm^{-1} to be the ν_2 fundamental, obtaining a ν_2 harmonic frequency of 256 cm^{-1},[5] consistent with our value. As the assignment for each peak in the SEVI spectra is unambiguous, the value of the ν_2 harmonic frequency obtained here is more robust, suggesting that their original assignment of the Raman spectra was correct.

CONCLUSIONS

High-resolution photoelectron spectra of thiozonide are reported. The ions are cooled to their ground vibrational state in a cryogenic ion trap and the photodetached electrons are detected with the high resolution of SEVI, allowing for an unambiguous assignment of the adiabatic transition and the electron affinity of S_3. By fitting the simulated spectrum to the experimental results, the structure of thiozonide is determined. The observed ν_1 frequencies are consistent with prior results, but a lower value is recommended for the ν_2 frequency of the neutral than that of the most recent value from resonance Raman spectroscopy.

AUTHOR INFORMATION

Corresponding Author

*E-mail: dneumark@berkeley.edu. Phone: 510-642-3635.

Present Addresses

[†](C.H.) Thermo Fisher Scientific, 28199 Bremen, Germany.

[‡](T.I.Y.) Aerodyne Research, Billerica, Massachusetts 01821, United States.

Notes

The authors declare no competing financial interest.

ACKNOWLEDGMENTS

This research is funded by the Air Force Office of Scientific Research under Grant No. FA9550-12-1-0160 and the Defense University Research Instrumentation Program (DURIP) under Grant No. FA9550-11-1-0300. C.H. thanks the German Academic Exchange Service (DAAD) for a postdoctoral scholarship. T.I.Y. thanks the National Science and Engineering Research Council of Canada (NSERC) for a postgraduate scholarship.

REFERENCES

(1) Meyer, B. Elemental Sulfur. *Chem. Rev.* **1976**, *76*, 367−388.

(2) Berkowitz, J.; Marquart, J. R. Equilibrium Composition of Sulfur Vapor. *J. Chem. Phys.* **1963**, *39*, 275−283.

(3) Brabson, G. D.; Mielke, Z.; Andrews, L. Infrared Spectra and Structure of Isotopically Enriched S_3 and S_4 in Solid Argon. *J. Phys. Chem.* **1991**, *95*, 79−86.

(4) Hassanzadeh, P.; Andrews, L. Vibronic Absorption Spectra of S_3 and S_4 in Solid Argon. *J. Phys. Chem.* **1992**, *96*, 6579−6585.

(5) Lenain, P.; Picquenard, E.; Lesne, J. L.; Corset, J. Raman Spectra of Overheated Sulfur Vapor. *J. Mol. Struct.* **1986**, *142*, 355−358.

(6) Picquenard, E.; Eljaroudi, O.; Corset, J. Resonance Raman Spectra of the S_3 Molecule in Sulphur Vapour. *J. Raman Spectrosc.* **1993**, *24*, 11−19.

(7) McCarthy, M. C.; Thorwirth, S.; Gottlieb, C. A.; Thaddeus, P. The Rotational Spectrum and Geometrical Structure of Thiozone, S_3. *J. Am. Chem. Soc.* **2004**, *126*, 4096−4097.

(8) Thorwirth, S.; McCarthy, M. C.; Gottlieb, C. A.; Thaddeus, P.; Gupta, H.; Stanton, J. F. Rotational Spectroscopy and Equilibrium Structures of S_3 and S_4. *J. Chem. Phys.* **2005**, *123*, 054326.

(9) Berkowitz, J.; Lifshitz, C. Photoionization of High-Temperature Vapors. II. Sulfur Molecular Species. *J. Chem. Phys.* **1968**, *48*, 4346−4350.

(10) Meyer, B.; Oommen, T. V.; Stroyerh., T. The Visible Spectrum of S_3 and S_4. *J. Mol. Spectrosc.* **1972**, *42*, 335−343.

(11) Carlsen, N. R.; Schaefer, H. F. Open (C_{2v}) and Closed (D_{3h}) Forms of the S_3 Molecule, Thiozone. *Chem. Phys. Lett.* **1977**, *48*, 390−392.

(12) Hohl, D.; Jones, R. O.; Car, R.; Parrinello, M. Structure of Sulfur Clusters Using Simulated Annealing: S_2 to S_{13}. *J. Chem. Phys.* **1988**, *89*, 6823−6835.

(13) Raghavachari, K.; Rohlfing, C. M.; Binkley, J. S. Structures and Stabilities of Sulfur Clusters. *J. Chem. Phys.* **1990**, *93*, 5862−5874.

(14) Rice, J. E.; Amos, R. D.; Handy, N. C.; Lee, T. J.; Schaefer, H. F. The Analytic Configuration Interaction Gradient Method: Application to the Cyclic and Open Isomers of the S_3 Molecule. *J. Chem. Phys.* **1986**, *85*, 963−968.

(15) Francisco, J. S.; Lyons, J. R.; Williams, I. H. High-Level ab Initio Studies of the Structure, Vibrational Spectra, and Energetics of S_3. *J. Chem. Phys.* **2005**, *123*, 054302.

(16) Peterson, K. A.; Lyons, J. R.; Francisco, J. S. An ab Initio Study of the Low-Lying Electronic States of S_3. *J. Chem. Phys.* **2006**, *125*, 084314.

(17) Chivers, T.; Drummond, I. Characterization of the Trisulfur Radical Anion S_3^- in Blue Solutions of Alkali Polysulfides in Hexamethylphosphoramide. *Inorg. Chem.* **1972**, *11*, 2525−2527.

(18) Chivers, T.; Lau, C. Raman Spectroscopic Identification of the S_4N^- and S_3^- Ions in Blue Solutions of Sulfur in Liquid Ammonia. *Inorg. Chem.* **1982**, *21*, 453−455.

(19) Clark, R. J. H.; Dines, T. J.; Kurmoo, M. On the Nature of the Sulfur Chromophores in Ultramarine Blue, Green, Violet, and Pink and of the Selenium Chromophore in Ultramarine Selenium: Characterization of Radical Anions by Electronic and Resonance Raman Spectroscopy and the Determination of Their Excited-State Geometries. *Inorg. Chem.* **1983**, *22*, 2766−2772.

(20) Chivers, T. Ubiquitous Trisulphur Radical Ion S_3^-. *Nature* **1974**, *252*, 32−33.

(21) Shnitko, I.; Fulara, J.; Garkusha, I.; Nagy, A.; Maier, J. P. Electronic Transitions of S_2^- and S_3^- in Neon Matrixes. *Chem. Phys.* **2008**, *346*, 8−12.

(22) Pokrovski, G. S.; Dubrovinsky, L. S. The S_3^- Ion Is Stable in Geological Fluids at Elevated Temperatures and Pressures. *Science* **2011**, *331*, 1052−1054.

(23) Nimlos, M. R.; Ellison, G. B. Photoelectron Spectroscopy of SO_2^-, S_3^-, and S_2O^-. *J. Phys. Chem.* **1986**, *90*, 2574−2580.

(24) Hunsicker, S.; Jones, R. O.; Gantefor, G. Rings and Chains in Sulfur Cluster Anions S^- to S_9^-: Theory (Simulated Annealing) and Experiment (Photoelectron Detachment). *J. Chem. Phys.* **1995**, *102*, 5917−5936.

(25) Handschuh, H.; Gantefor, G.; Eberhardt, W. Vibrational Spectroscopy of Clusters Using a "Magnetic Bottle" Electron Spectrometer. *Rev. Sci. Instrum.* **1995**, *66*, 3838−3843.

(26) Osterwalder, A.; Nee, M. J.; Zhou, J.; Neumark, D. M. High Resolution Photodetachment Spectroscopy of Negative Ions via Slow Photoelectron Imaging. *J. Chem. Phys.* **2004**, *121*, 6317−6322.

(27) Hock, C.; Kim, J. B.; Weichman, M. L.; Yacovitch, T. I.; Neumark, D. M. Slow Photoelectron Velocity-Map Imaging Spectroscopy of Cold Negative Ions. *J. Chem. Phys.* **2012**, *137*, 244201.

(28) Neumark, D. M. Slow Electron Velocity-Map Imaging of Negative Ions: Applications to Spectroscopy and Dynamics. *J. Phys. Chem. A* **2008**, *112*, 13287−13301.

(29) Even, U.; Jortner, J.; Noy, D.; Lavie, N.; Cossart-Magos, C. Cooling of Large Molecules Below 1 K and He Clusters Formation. *J. Chem. Phys.* **2000**, *112*, 8068−8071.

(30) Gerlich, D. Inhomogeneous RF Fields: A Versatile Tool for the Study of Processes with Slow Ions. In *Advances in Chemical Physics*; Ng, C.-Y., Baer, M., Eds.; John Wiley & Sons, Inc.: Hoboken, NJ, 1992; Vol. *82*, pp 1−176.

(31) Eppink, A.; Parker, D. H. Velocity Map Imaging of Ions and Electrons Using Electrostatic Lenses: Application in Photoelectron and Photofragment Ion Imaging of Molecular Oxygen. *Rev. Sci. Instrum.* **1997**, *68*, 3477−3484.
(32) Hansen, E. W.; Law, P. L. Recursive Methods for Computing the Abel Transform and Its Inverse. *J. Opt. Sci. Am. A* **1985**, *2*, 510−520.
(33) Garand, E.; Neumark, D. M. Study of RgS^- and RgS (Rg = Ne, Ar, and Kr) via Slow Photoelectron Velocity-Map Imaging Spectroscopy and ab Initio Calculations. *J. Chem. Phys.* **2011**, *135*, 024302.
(34) Blondel, C.; Chaibi, W.; Delsart, C.; Drag, C. The Fine Structure of S and S^- Measured with the Photodetachment Microscope. *J. Phys. B: At. Mol. Opt. Phys.* **2006**, *39*, 1409−1416.
(35) Knowles, P. J.; Hampel, C.; Werner, H.-J. Coupled Cluster Theory for High Spin, Open Shell Reference Wave Functions. *J. Chem. Phys.* **1993**, *99*, 5219−5227.
(36) Deegan, M. J. O.; Knowles, P. J. Perturbative Corrections to Account for Triple Excitations in Closed and Open Shell Coupled Cluster Theories. *Chem. Phys. Lett.* **1994**, *227*, 321−326.
(37) Dunning, T. H.; Peterson, K. A.; Wilson, A. K. Gaussian Basis Sets for Use in Correlated Molecular Calculations. X. The Atoms Aluminum Through Argon Revisited. *J. Chem. Phys.* **2001**, *114*, 9244−9253.
(38) Werner, H.-J.; Knowles, P. J.; Knizia, G.; Manby, F. R.; Schütz, M. *MOLPRO*, version 2010.1, a package of ab initio programs; Cardiff University: Cardiff, U.K., 2010.
(39) Mozhayskiy, V. A.; Krylov, A. I. ezSpectrum. http://iopenshell.usc.edu/downloads.
(40) Duschinsky, F. The Importance of the Electron Spectrum in Multi Atomic Molecules. Concerning the Franck−Condon Principle. *Acta Physicochim. URSS* **1937**, *7*, 551−566.
(41) Cooper, J.; Zare, R. N. Angular Distribution of Photoelectrons. *J. Chem. Phys.* **1968**, *48*, 942−943.
(42) Mabbs, R.; Grumbling, E. R.; Pichugin, K.; Sanov, A. Photoelectron Imaging: An Experimental Window into Electronic Structure. *Chem. Soc. Rev.* **2009**, *38*, 2169−2177.
(43) Ellis, H. B.; Ellison, G. B. Photoelectron Spectroscopy of HNO^- and DNO^-. *J. Chem. Phys.* **1983**, *78*, 6541−6558.
(44) Nimlos, M. R.; Harding, L. B.; Ellison, G. B. The Electronic States of Si_2 and Si_2^- As Revealed by Photoelectron Spectroscopy. *J. Chem. Phys.* **1987**, *87*, 5116−5124.
(45) Jones, R. O.; Gantefor, G.; Hunsicker, S.; Pieperhoff, P. Structure and Spectroscopy of Phosphorus Cluster Anions: Theory (Simulated Annealing) and Experiment (Photoelectron Detachment). *J. Chem. Phys.* **1995**, *103*, 9549−9562.
(46) Zhou, J.; Garand, E.; Eisfeld, W.; Neumark, D. M. Slow Electron Velocity-Map Imaging Spectroscopy of the 1-Propynyl Radical. *J. Chem. Phys.* **2007**, *127*, 034304.
(47) Garand, E.; Yacovitch, T. I.; Neumark, D. M. Slow Photoelectron Imaging Spectroscopy of CCO^- and CCS^-. *J. Chem. Phys.* **2008**, *129*, 074312.
(48) Wester, R. Radiofrequency Multipole Traps: Tools for Spectroscopy and Dynamics of Cold Molecular Ions. *J. Phys. B: At. Mol. Opt. Phys.* **2009**, *42*, 154001.
(49) Boyarkin, O. V.; Mercier, S. R.; Kamariotis, A.; Rizzo, T. R. Electronic Spectroscopy of Cold, Protonated Tryptophan and Tyrosine. *J. Am. Chem. Soc.* **2006**, *128*, 2816−2817.
(50) Wang, X. B.; Wang, L. S. Development of a Low-Temperature Photoelectron Spectroscopy Instrument Using an Electrospray Ion Source and a Cryogenically Controlled Ion Trap. *Rev. Sci. Instrum.* **2008**, *79*, 073108.
(51) Asmis, K. R.; Brummer, M.; Kaposta, C.; Santambrogio, G.; von Helden, G.; Meijer, G.; Rademann, K.; Woste, L. Mass-Selected Infrared Photodissociation Spectroscopy of $V_4O_{10}^+$. *Phys. Chem. Chem. Phys.* **2002**, *4*, 1101−1104.
(52) Garand, E.; Kamrath, M. Z.; Jordan, P. A.; Wolk, A. B.; Leavitt, C. M.; McCoy, A. B.; Miller, S. J.; Johnson, M. A. Determination of Noncovalent Docking by Infrared Spectroscopy of Cold Gas-Phase Complexes. *Science* **2012**, *335*, 694−698.
(53) Brannon, P. J.; Church, C. H.; Peters, C. W. Electric Field Induced Spectra of Molecular Hydrogen, Deuterium and Deuterium Hydride. *J. Mol. Spectrosc.* **1968**, *27*, 44−54.
(54) Wigner, E. P. On the Behavior of Cross Sections Near Thresholds. *Phys. Rev.* **1948**, *73*, 1002−1009.